Investigation of Sheet Metals Subjected to Simultaneous Embossing on Both Sides Utilizing Multiple Punches

Consorcio S. Namoco, Jr.*
College of Industrial and Information Technology
Mindanao University of Science and Technology
CM Recto Ave., Lapasan, Cagayan de Oro City, 9000 Philippines
**csnamoco@must.edu.ph*

Date received: July 1, 2013
Revision accepted: October 10, 2013

Abstract

In this study, an innovative technique of embossing process of sheet metal is presented. Such technique involves simultaneous embossing on both sides utilizing multiple punches. This technique has advantages over the embossing method conducted in one side of the sheet only utilizing a die. In embossing with a die, since only one side of the sheet is being processed, the residual stress in both sides of the embossed sheet is different, and it may cause warp to occur. Moreover, decreasing the pitch between emboss is restricted or limited with the tool and die used in forming.

In an attempt to overcome these limitations, a process that performs embossing simultaneously on both sides utilizing multiple punches has been explored. In this study, simultaneous embossing on both sides of soft aluminum has been conducted and the mechanical properties of the embossed sheet are then investigated. Results showed that the bending rigidity of the embossed specimen increases with the emboss height. It was found out that the value of tensile strength and total elongation has no appreciable difference from that of plain sheet at θ=45^0 *direction.*

Keywords: sheet metal, simultaneous embossing, bending strength, tensile strength, FEM simulation

1. Introduction

Weight reduction, improvement in energy and resources savings and lowering of cost are some of the pressing concerns of the sheet metal industry nowadays. One of the practical ways to address these issues is to utilize a sheet metal of thinner gages. However, in using a lighter grade conventional sheet metal during press forming, several problems arise such

as decrease in rigidity and structural strength. Also, the formability of the sheet decreases with decreasing sheet thickness (Yamaguchi and Mellor, 1976; Yamaguchi *et al.* 1987).

The metal panel's stiffness and rigidity can be increased by performing an embossing technique on the sheet. In previous studies (Namoco *et al*., 2007), embossing was conducted in only one side of the sheet utilizing a die. This process has the advantage of being easy to perform but, on the other hand, residual stress in both sides is different causing warp to occur. Moreover, decreasing the pitch between emboss is limited with the tool and die. Hence, to overcome these problems, a process that performs embossing simultaneously on both sides utilizing multiple punches is investigated. In this study, simultaneous embossing on both sides of soft aluminum sheet is conducted and the mechanical properties and characteristics of the embossed sheet are then examined.

2. Methodology

2.1 Experimental Set-up for Simultaneous Embossing on Both Sides

Soft aluminum (A1050P) sheet with a thickness of 1.0mm is used as test specimen. In Figure 1, the schematic of experimental device used for this forming technique is shown. Multiple punches are arranged in the upper and lower parts of the device. Embossing is conducted by allowing the upper tool to move downward while the lower tool remained fixed. The sheet blank is placed in a holder. The punches in the upper and lower tools with a diameter of 6.0 mm are arranged with an interval of 10mm. Embossing is completed by repeating the process while moving the specimen at intervals equal to the distance between punches.

The experiment is conducted with an emboss height, h, of 0.5mm to 2.0mm. Figure 2 shows the details of the embossing process. The experimental conditions used are shown in Table 1. The embossing direction, θ, is changed by changing the arrangement of punches. Figure 3 shows the schematic of emboss direction used in the experiment. Figure 4 shows photographs of embossed specimens demonstrating that such forming technique can be carried out successfully.

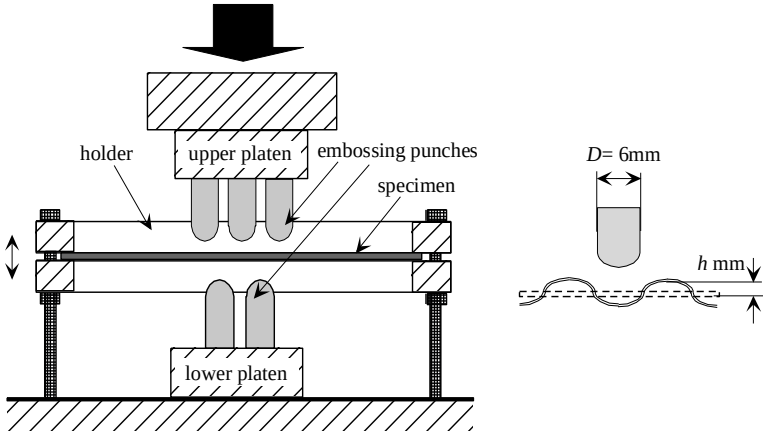

Figure 1. Schematic of the embossing device used in the experiment

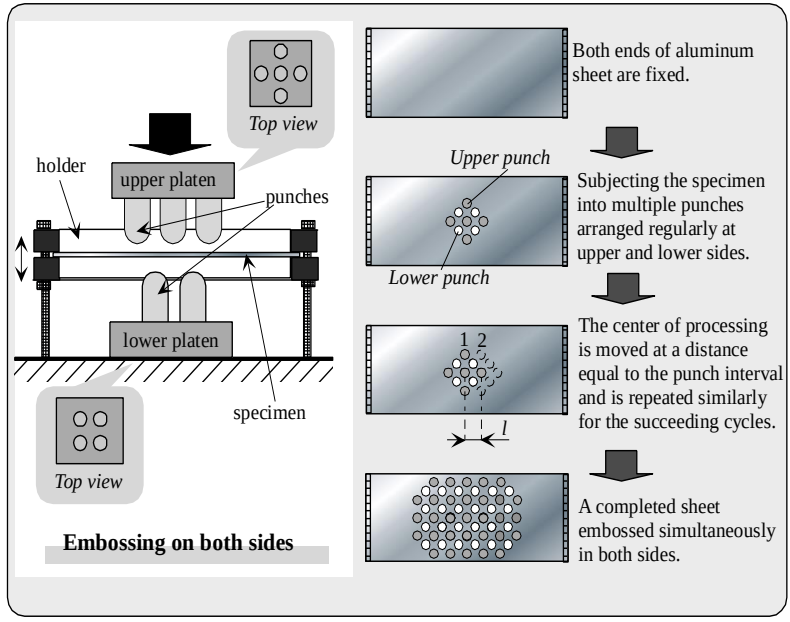

Figure 2. Details of the embossing technique

Table 1. Experimental conditions on simultaneous embossing on both sides

	A1050P
Thickness, t (mm)	1.0
Punch diameter, D (mm)	6.0
Emboss hiegth, h (mm)	0.5, 1.0 1.5, 2.0
Emboss direction, θ (deg)	0, 45

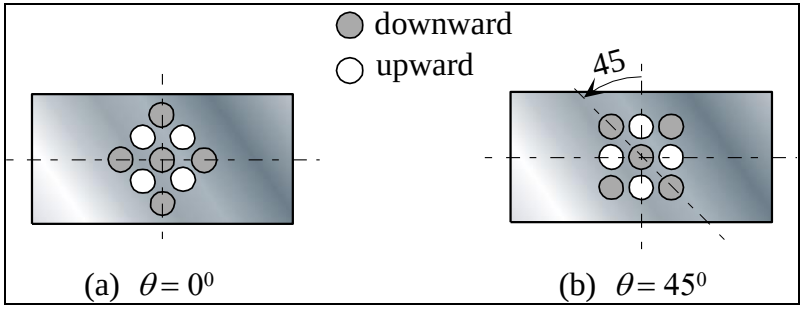

Figure 3. Schematic of emboss direction, θ used in the experiment

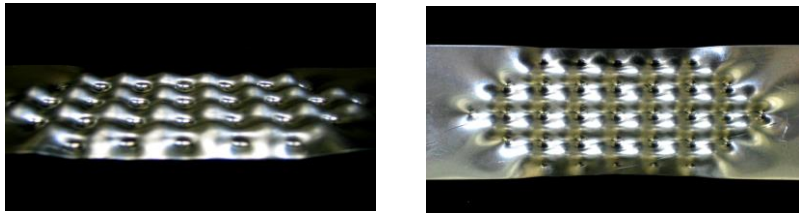

Figure 4. Specimens embossed at both sides

2. 2 Bending Characteristics of the Embossed Sheet

2.2.1 Bending Specimen and Bending Test Method

Bending test specimens with dimensions of 30mm x 140mm are first subjected to embossing on both sides simultaneously. Figure 5 shows the embossed specimens at $\theta = 0^0$ and 45^0 directions for bending test. Three-

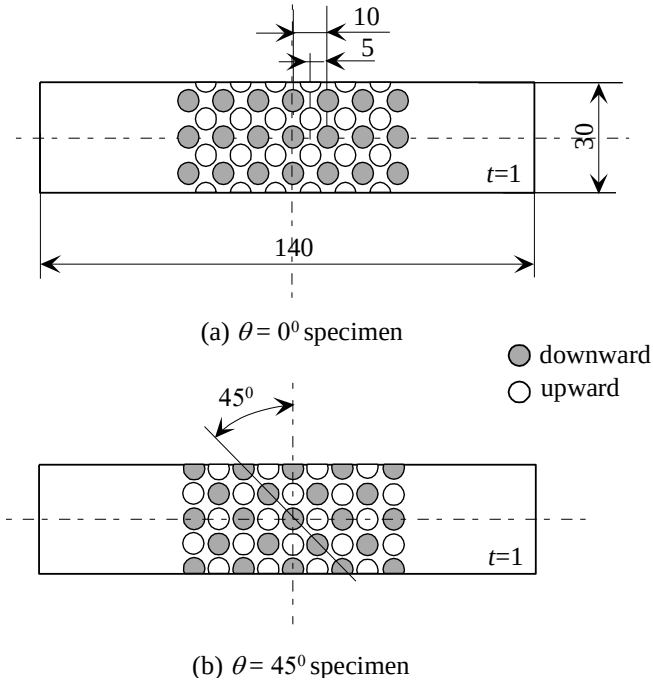

Figure 5. Geometry of bending test specimens (in mm)

point bending test is then conducted as shown in Figure 6. The load is applied using a cylindrical punch along the center of the embossed specimen.

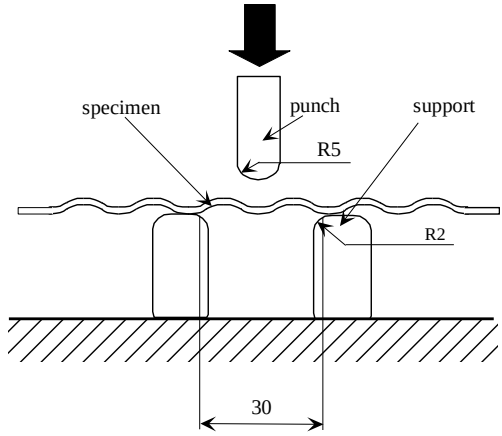

Figure 6. Bending test set-up (in mm)

2.2.2 Finite Element Method (FEM) Simulation of the Bending Test

Numerical simulations of embossing, and bending tests have conducted utilizing the explicit finite element code LS-DYNA3D (Hallquist, 2003). The multi-purpose software JVISION (JVISION User's Manual, 2003) is used to create the finite element mesh and assign the boundary conditions. To reduce computational time and expense, symmetry is being taken advantage, hence, only one quarter of the geometry is considered. The finite element models are established according to the dimensions used in the experiments. The FEM mesh for the blank and embossing punch are shown in Figure 7 and Figure 8, respectively. In Figure 9, the quarter model for the embossing process is shown. The geometry and condition for bending test simulations are similar with that of the experiment. The mesh size in the emboss area is 0.3mm. The sheet blank is meshed using shell elements with Belytschko-Tsay element formulation and five integration points through the thickness. The simulations are performed using the Barlat (Barlat and Lain, 1989) constitutive model as implemented in LS-DYNA3D. This material model uses the Lankford parameters (R_0, R_{45}, R_{90}) for the definition of anisotropy. The embossing punches, holder, bending punch and supports are created using rigid materials. The material properties used in the analysis which are derived from uniaxial tests are reported in Table 2. The coefficient of friction used is 0.2. In the simulation of bending tests, the restart input data method is used. The full deck restart has the capability to redefine contact surfaces, add new contact surfaces, replace or add parts, and many others. In the full restart analysis, the stresses, strains, displacements, and analysis time from previous analysis are carried over.

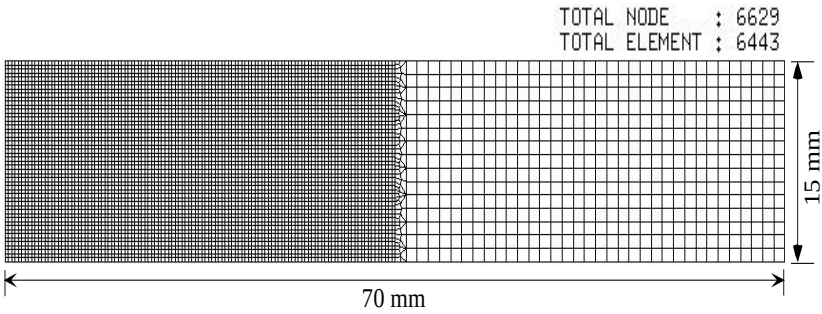

Figure 7. FEM mesh for sheet blank (quarter model)

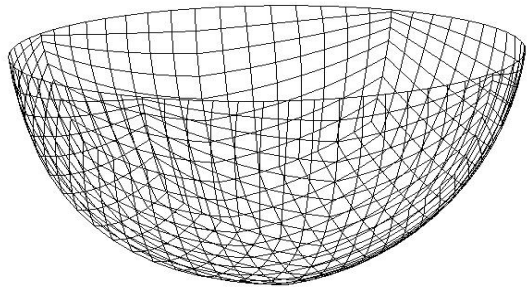

Figure 8. FEM mesh for embossing punch

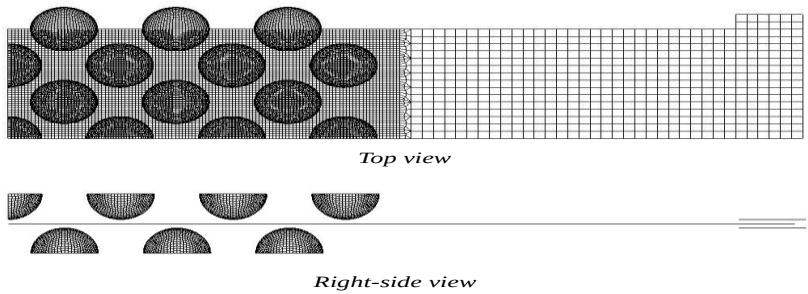

Figure 9. Quarter model of embossing set-up used in simulation

Table 2 Material properties for A1050P used in the analysis

	A1050P
Yield strength, σ_{ys} (MPa)	30.0
Young's modulus, E (GPa)	69.0
Poisson's ratio, v	0.33
Strength coefficient, k (MPa)	145
Work hardening coefficient, n	0.26
r – value, R_0	0.57
r – value, R_{45}	1.0
r – value, R_{90}	0.57

2.3 Tensile Characteristics of the Embossed Sheet

2.3.1 Tensile Test Specimen

Tensile test is performed with specimens subjected to this embossing technique. Specimens are prepared in such a way that the loading direction is the same with the rolling direction of raw sheet in accordance with the Japan Industrial Standard (JIS). Embossing of the tensile specimens are performed at an embossing direction, $\theta = 0^0$ and 45^0 as shown in Figure 10. The tensile test is conducted at a speed of 1mm/min.

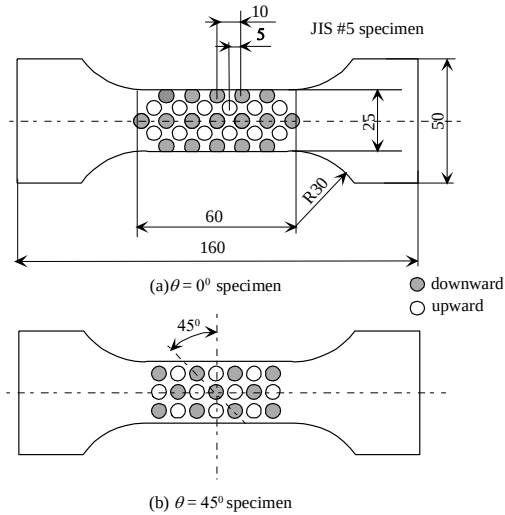

Figure 10. Geometry of tensile test specimens (in mm)

3. Results and Discussion

3.1 Von Mises Equivalent Stress and Equivalent Plastic Strain Distributions

Figure 11 and Figure 12 show the von Mises equivalent stress and equivalent plastic strain distributions for $\theta = 0^0$ and $\theta = 45^0$ specimens, respectively, embossed at h=2.0mm. As can be observed from the figures, the regions where the equivalent stress and strain are at largest, occur in the center of the emboss region, whether downward or upward emboss, as expected.

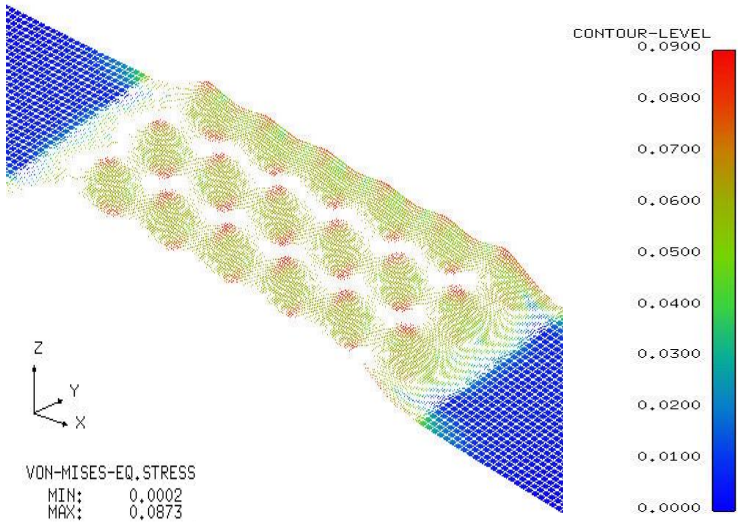

(a) von Mises equivalent stress ($\theta = 0^0$)

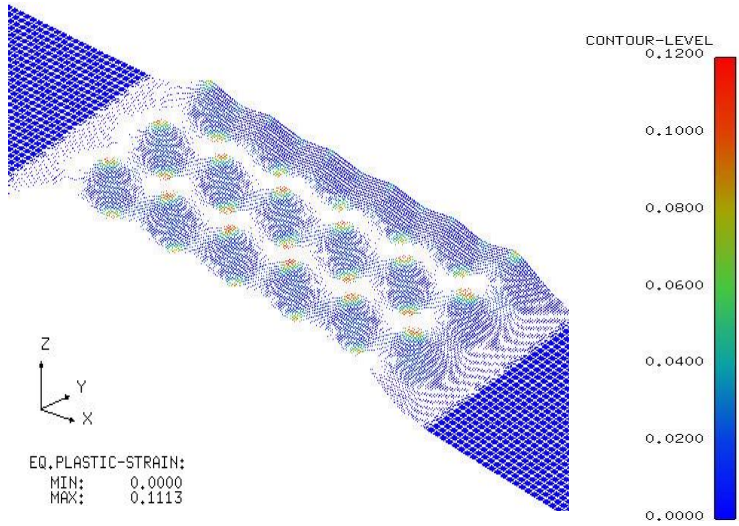

(b) Equivalent plastic strain ($\theta = 0^0$)

Figure 11. The von Mises equivalent stress and equivalent plastic strain distributions for $\theta = 0^0$ specimen. (h=2.0mm)

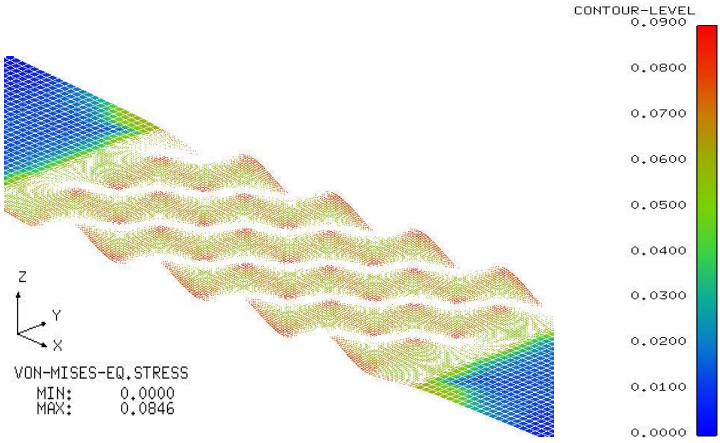

(a) von Mises equivalent stress ($\theta = 45^0$)

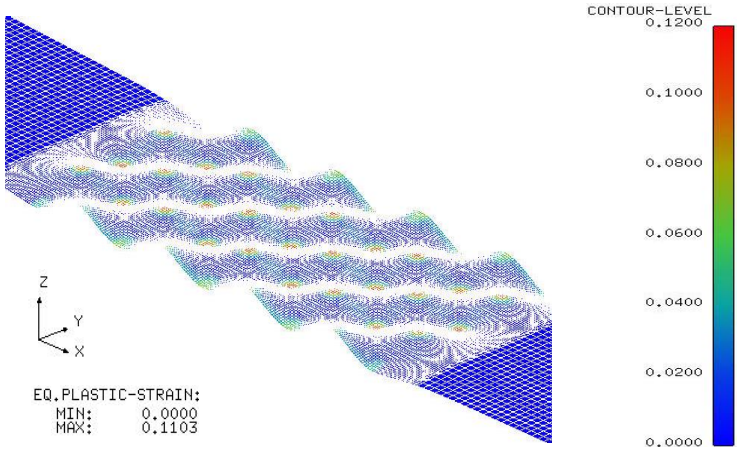

(b) Equivalent plastic strain ($\theta = 45^0$)

Figure 12. The von Mises equivalent stress and equivalent plastic strain distributions for $\theta = 45^0$ specimen. (h=2.0mm)

3.2 Evaluation of Bending Properties of Embossed Sheet

Figure 13 shows the experimental and numerical results of the bending tests for $\theta = 0^0$ and $\theta = 45^0$ specimens. The FEM simulation results are in good correlation with the experiments. The load–deflection curves show that the

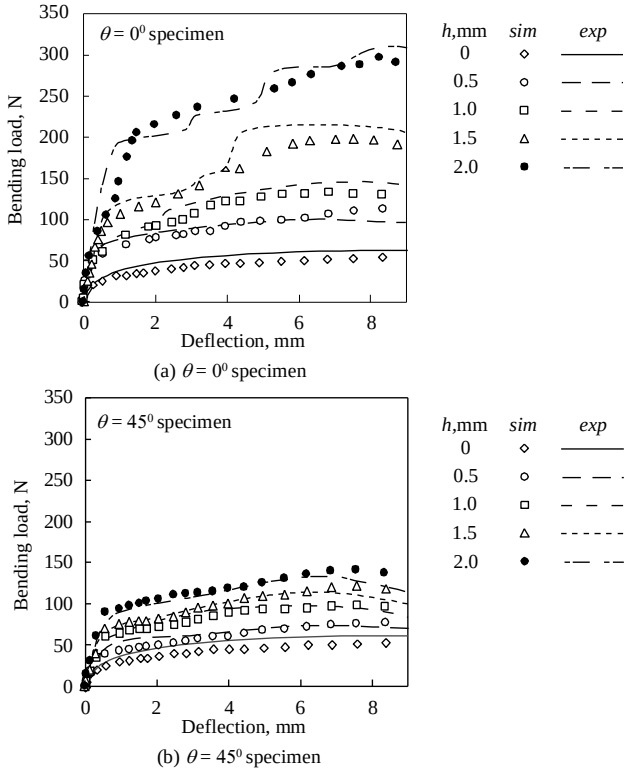

Figure 13. Bending load - deflection curves

technique is an effective way in increasing the rigidity of the sheet. As shown in the figure, the emboss direction, θ, has a great influence on the bending rigidity of the embossed sheet. With $\theta = 0^0$ specimen, the increase in section modulus of the specimen is at maximum, hence, increasing the moment of inertia. Moreover, the load is distributed among the emboss due to greater area of contact between the punch and the embossed sheet. For both specimens, the bending loads required to deflect the specimen increases as the emboss height is increased. Considering the value of maximum bending load as the measure of bending strength, it can be observed that the bending strength of the emboss sheet increases with emboss height as shown in Figure 14. This can be attributed to the change in the cross-sectional shape of the specimen that increases the moment of inertia as well as to the strengthening effect due to the plastic deformation that is locally introduced in the emboss area.

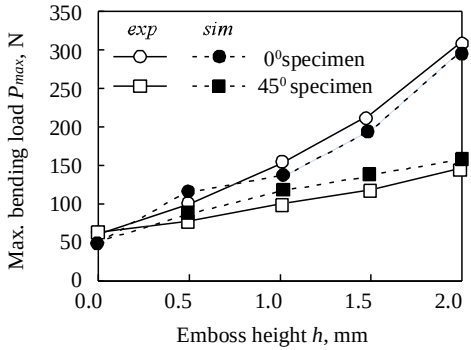

Figure 14. Influence of emboss height on the bending strength

3.2 Evaluation of Tensile Properties of Embossed Sheet

Figure 15 shows the nominal stress – nominal strain diagram of the embossed specimens at various emboss height in θ=0^0 and 45^0 directions. It can be observed that the tensile properties such as yield strength, tensile strength and total elongation, of the specimens subjected to embossing at both sides change considerably as compared to that of plain sheet specimen.

Figure 16 shows the relationship between the emboss height and tensile strength. For θ=45^0 specimen, the value of tensile strength does not change with emboss height and its value is almost the same with that of the plain sheet. For θ=0^0 specimen, on the other hand, at lower emboss heights (say, less than 1mm), the tensile strength does not vary substantially with that of the plain sheet but as the emboss height is increased, the tensile strength decreases.

In Figure 17, the relationship between the emboss height and total elongation is shown. As can be observed from the figure, there is a similar behavior with tensile strength and total elongation for θ = 0^0 and 45^0 specimens.

Figure 18 shows the photos of fractured specimens after the tensile test of specimen embossed at h=1.5mm. In the case of θ =0^0 specimen, fracture occurs across the head of the emboss due to the decrease in sheet thickness in the emboss area. It is in this direction wherein the change in shape of the specimen after embossing is at maximum. This decrease in thickness is considered to be responsible for the observed decrease in tensile strength and total elongation at higher emboss height for θ=0^0 specimen.

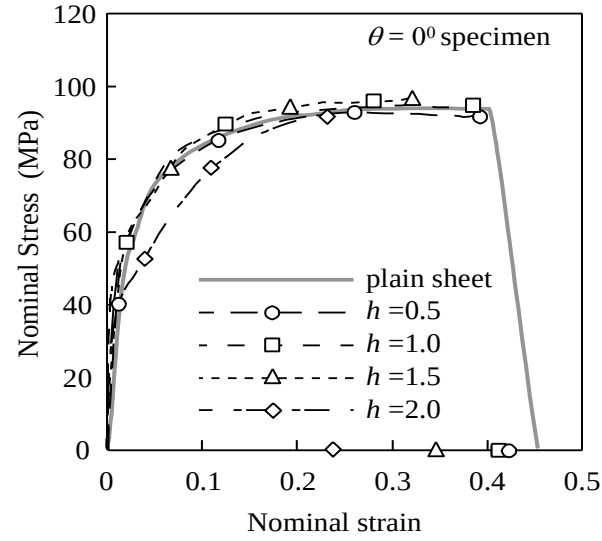

(a) $\theta = 0^0$ specimen

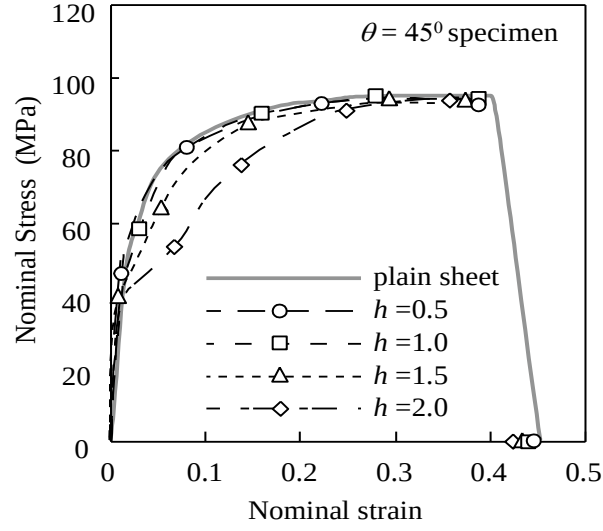

(b) $\theta = 45^0$ specimen

Figure 15. Nominal stress - nominal strain diagrams

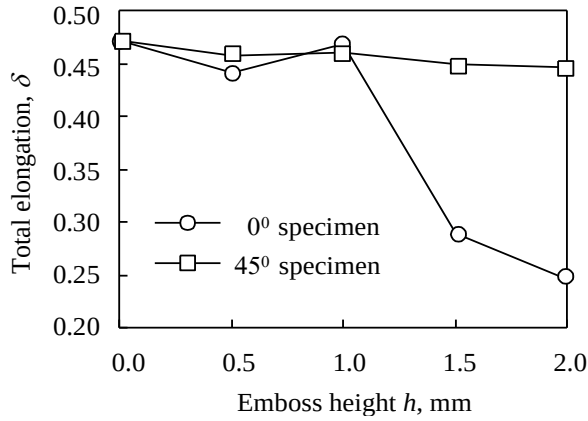

Figure 16. Influence of emboss height on total elongation

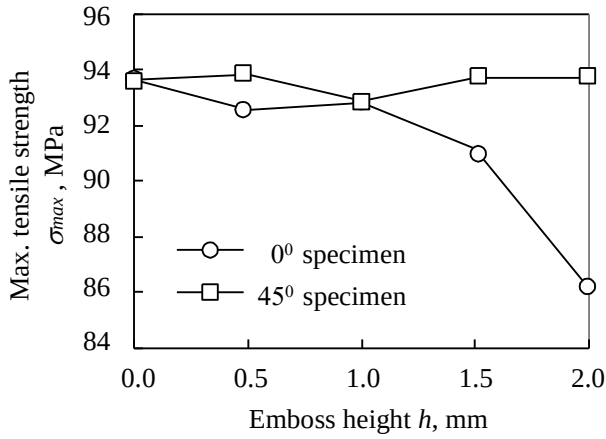

Figure 17. Influence of emboss height on tensile strength

4. Conclusion

In this study, embossing of Al-O sheet in both sides simultaneously has been investigated. In the bending test, it is confirmed that the maximum bending load and consequently, the bending rigidity, increases with the emboss height. The value is higher at $\theta=0^0$ than at $\theta=45^0$. FEM and experimental results in bending tests were in good agreement. In the tensile test, for $\theta=45^0$

specimen, the value of tensile strength and total elongation has no appreciable difference from that of plain sheet. For $\theta=0^0$ specimen, as the emboss height is increased, the tensile strength and total elongation correspondingly decrease.

5. References

Barlat F. and Lain, J.I. (1989) "Plastic behavior and stretchability of sheet metals, part I", *Int. J. Plasticity*, 5, 51-56.

Hallquist, J.O. (2003). *LS-DYNA Keyword User's Manual*, Livermore Software Technology Corporation.

JVISION User's Manual Ver. 2.5. 2003: The Japan Research Institute, Limited, Japan.

Namoco Jr. C.S., Iizuka, T., Hatanaka, N., Takakura, N., and Yamaguchi, K. (2007). Key Engineering Materials, Vol. 340, 377-382.

Namoco Jr. C.S., Iizuka, T., Hatanaka N., Takakura N., Yamaguchi, K. and Mater, J. (2007). Process. Tech, Vol. 192-193, 18-26.

Yamaguchi K., and Mellor P.B., (1976) Int. J. Mech.Sci., Vol.18, 85-90.

Yamaguchi K., Takakura N. and Fukuda, M. (1987) in: Proc. of the 2nd ICTP, 1267–1274.